

**Supporting information for**

**Theoretical Insight into the Redox-switchable Activity of Group 4 Metal Complexes for the Ring-Opening Polymerization of  $\epsilon$ -Caprolactone**

Xiaowei Xu,<sup>a</sup> Gen Luo,<sup>a,\*</sup> Zhaomin Hou,<sup>b</sup> Paula L. Diaconescu,<sup>c,\*</sup> Yi Luo<sup>a,\*</sup>

**Table of contents**

<b>Fig. S1</b> (a) SOMO of the three oxidized active species (isovalue = 0.04) and (b) Mulliken spin densities (isovalue = 0.003) of the three oxidized active species .....	S2
<b>Fig. S2</b> Relaxed potential energy surface (PES) scan for the dihedral angel of Ti-O1-C-O2 (step size = 10°, number of steps = 8) of $2_a^{ox}$ / $2_a^{red}$ at the DFT/BSI level .....	S2
<b>Fig. S3</b> Optimized structures (distances in Å) and distortion/interaction analysis of $TS3a^{ox}$ and $TS3a^{red}$ . Values in parentheses are the relative Gibbs free energy barriers. Energies are given in kcal mol <sup>-1</sup> .....	S2
<b>Fig. S4</b> Mulliken charges of the catalytic metal center in the stationary points involved in the $a^{ox}$ and $a^{red}$ mediated reaction pathways.....	S3
<b>Fig. S5</b> Optimized structures (distances in Å) and energies (kcal mol <sup>-1</sup> ) of the insertion and ring-opening products $4_b^{ox}$ and $4_b^{red}$ of the first monomer. Values in parentheses are the Gibbs free energies (kcal mol <sup>-1</sup> ) in solution relative to the isolated reactants.....	S3
<b>Fig. S6</b> Optimized structures (distances in Å) of the coordination complexes $1_b^{ox}$ vs $1_b^{red}$ and $5_b^{ox}$ vs $5_b^{red}$ .....	S4
<b>Fig. S7</b> Mulliken charges on the catalytic metal center of the stationary points involved in the $b^{ox}$ and $b^{red}$ mediated reaction pathways. ....	S7
<b>Fig. S8</b> Optimized structures (distances in Å) and distortion/interaction analysis (kcal mol <sup>-1</sup> ) of the four key transition states ( $TS1_c^{ox}$ vs $TS1_c^{red}$ , $TS3_c^{ox}$ vs $TS3_c^{red}$ ). Values in parentheses are the relative free energy barriers in solution (kcal mol <sup>-1</sup> ).....	S5
<b>Fig. S9</b> Optimized structure (distances in Å) and energy (kcal mol <sup>-1</sup> ) of the insertion and ring-opening products $4_c^{ox}$ and $4_c^{red}$ of the first monomer. Values in parentheses are the relative Gibbs free energies (kcal mol <sup>-1</sup> ) with respect to the sum of isolated reactants.....	S5
<b>Fig. S10</b> Optimized structures (distances in Å) of transition states $TS4_c^{ox}$ and $TS4_c^{red}$ . Values in parentheses are the relative Gibbs free energies (kcal mol <sup>-1</sup> ) in solution with respect to isolated reactants.....	S6
<b>Fig. S11</b> Mulliken charges of the catalytic metal center in the stationary points involved in the $c^{ox}$ and $c^{red}$ mediated reaction pathways. ....	S6
<b>Fig. S12</b> Free energy profiles for possible pathway of ROP of CL with C=O bond cleavage mediated by $b^{ox}$ and $b^{red}$ . ....	S7
<b>Table S1</b> Wiberg bond orders in $b^{red}$ , $c^{red}$ , $b^{ox}$ , and $c^{ox}$ .....	S7
<b>Table S2</b> Relative electronic energies ( $\Delta E$ , kcal/mol) of various spin states of active species. ....	S8
Examples of the input files .....	S9

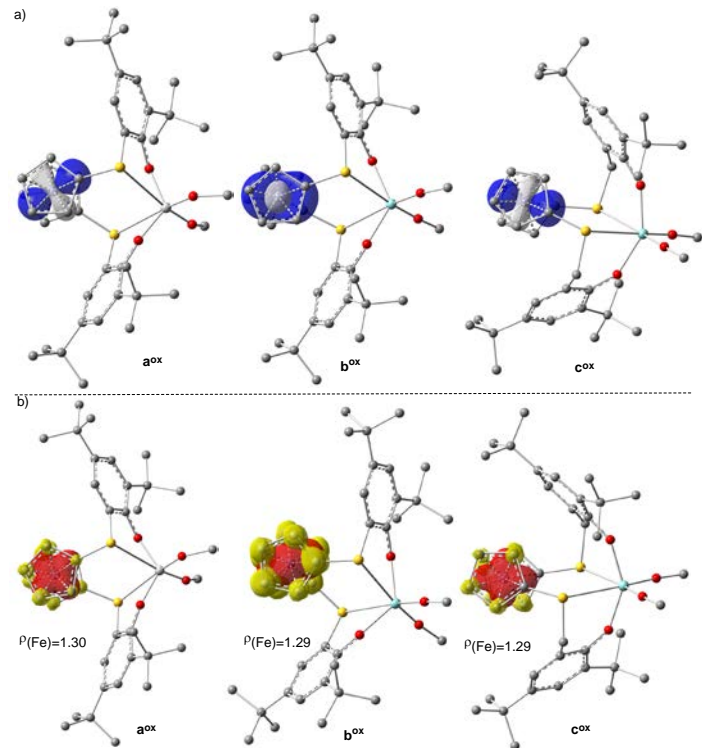


**Fig. S1** (a) SOMO of the three oxidized active species (isovalue = 0.04) and (b) Mulliken spin densities (isovalue = 0.003) of the three oxidized active species.

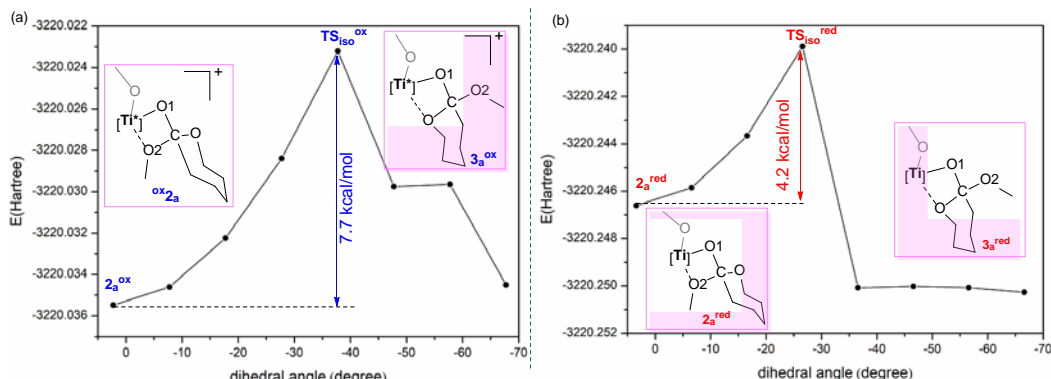


**Fig. S2** Relaxed potential energy surface (PES) scan for the dihedral angel of Ti-O1-C-O2 (step size =  $10^\circ$ , number of steps = 8) of  $2_a^{ox}$ / $2_a^{red}$  at the DFT/BSI level.

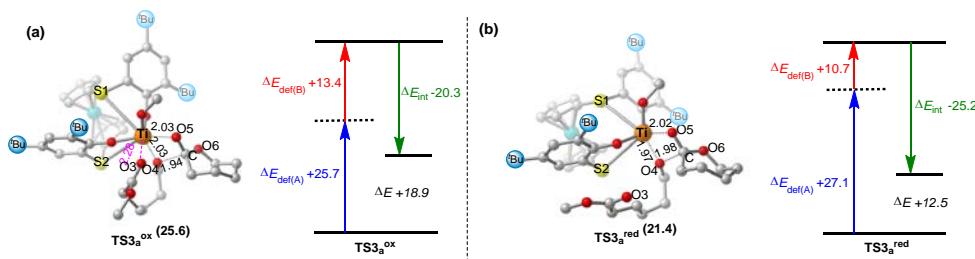


**Fig. S3** Optimized structures (distances in Å) and distortion/interaction analysis of  $TS3a^{ox}$  and  $TS3a^{red}$ . Values in parentheses are the relative Gibbs free energy barriers. Energies are given in kcal mol<sup>-1</sup>.

The energy distortion/interaction analyses (Fig. S3) of the transition states **TS3<sub>a</sub><sup>red</sup>** and **TS3<sub>a</sub><sup>ox</sup>** show that the interaction energy ( $\Delta E_{\text{int}}$ ) between the incoming CL moiety and the remaining metal complex mainly accounts for the stability difference between the two transition states ( $-20.3 \text{ kcal mol}^{-1}$  for **TS3<sub>a</sub><sup>ox</sup>** vs  $-25.2 \text{ kcal mol}^{-1}$  for **TS3<sub>a</sub><sup>red</sup>**, Fig. 5). The more negative value of  $\Delta E_{\text{int}}$  for **TS3<sub>a</sub><sup>red</sup>** could be ascribed to the existence of an additional chelation effect between the metal center and the carbonyl oxygen ( $\text{Ti}\cdots\text{O}3 = 2.28 \text{ \AA}$ ) that relatively weakens the interaction between the metal center and the incoming CL moiety ( $\text{Ti}\cdots\text{O}5 = 2.03 \text{ \AA}$  and  $\text{C}\cdots\text{O}4 = 1.94 \text{ \AA}$ , Fig. S3) due to steric properties.

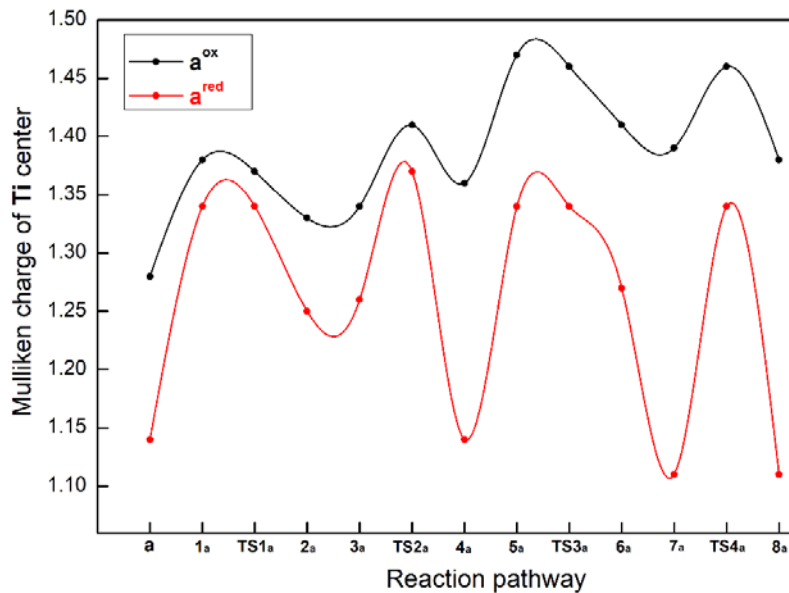


**Fig. S4** Mulliken charges on the catalytic metal center in the stationary points involved in the **a<sup>ox</sup>** and **a<sup>red</sup>** mediated reaction pathways.

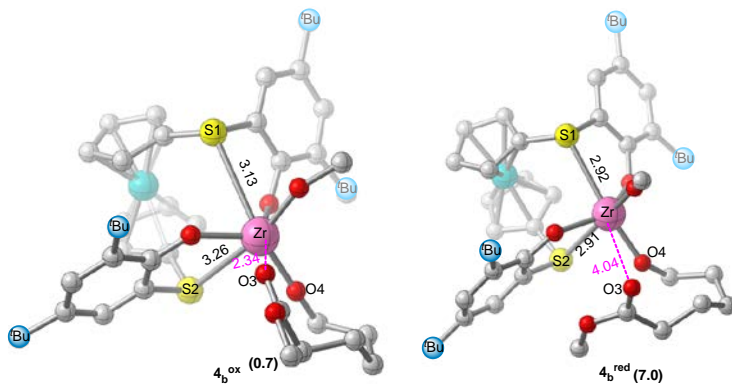


**Fig. S5** Optimized structures (distances in  $\text{\AA}$ ) and energies ( $\text{kcal mol}^{-1}$ ) of the insertion and ring-opening products **4<sub>b</sub><sup>ox</sup>** and **4<sub>b</sub><sup>red</sup>** of the first monomer. Values in parentheses are the Gibbs free energies ( $\text{kcal mol}^{-1}$ ) in solution relative to the isolated reactants.

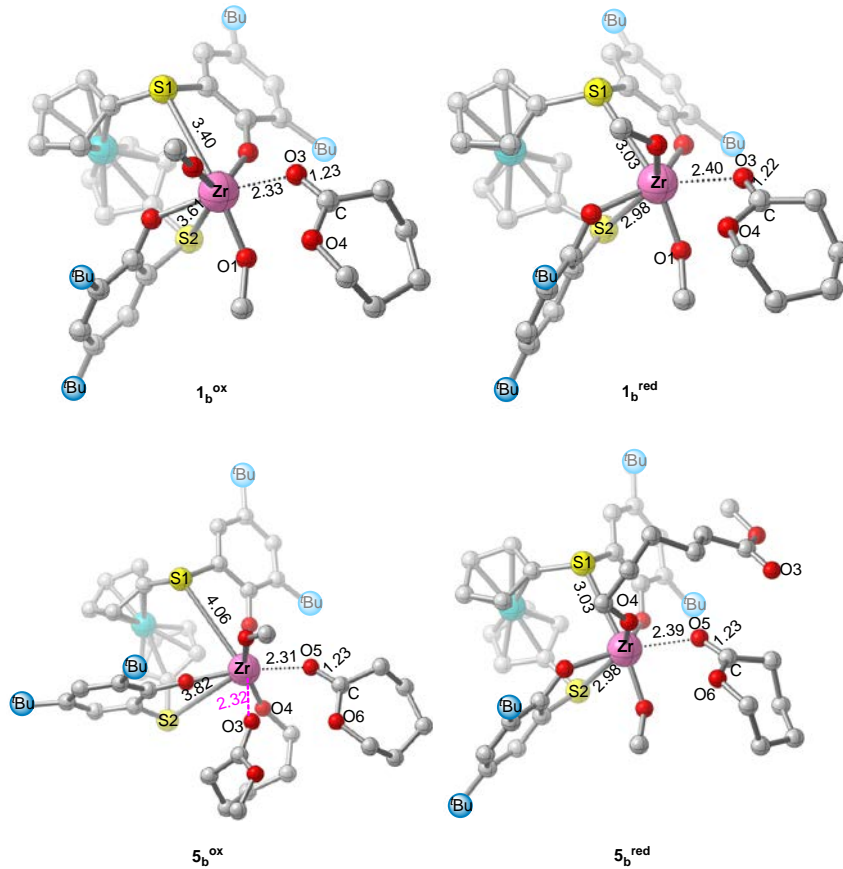


**Fig. S6** Optimized structures (distances in Å) of the coordination complexes **1<sub>b</sub><sup>ox</sup>** vs **1<sub>b</sub><sup>red</sup>** and **5<sub>b</sub><sup>ox</sup>** vs **5<sub>b</sub><sup>red</sup>**.

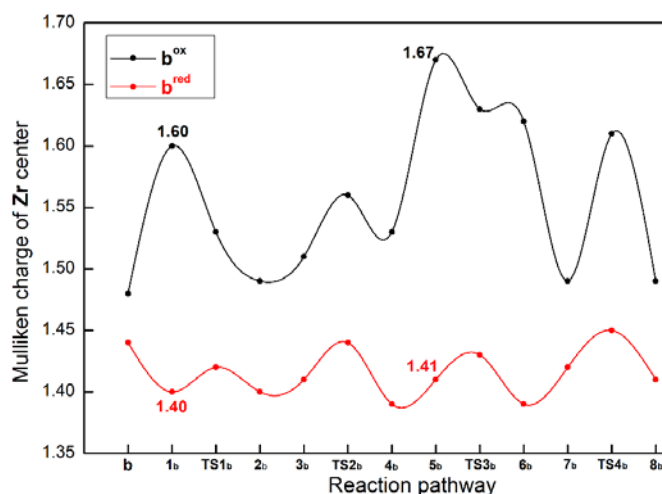


**Fig. S7** Mulliken charges on the catalytic metal center of the stationary points involved in the **b<sup>ox</sup>** and **b<sup>red</sup>** mediated reaction pathways.

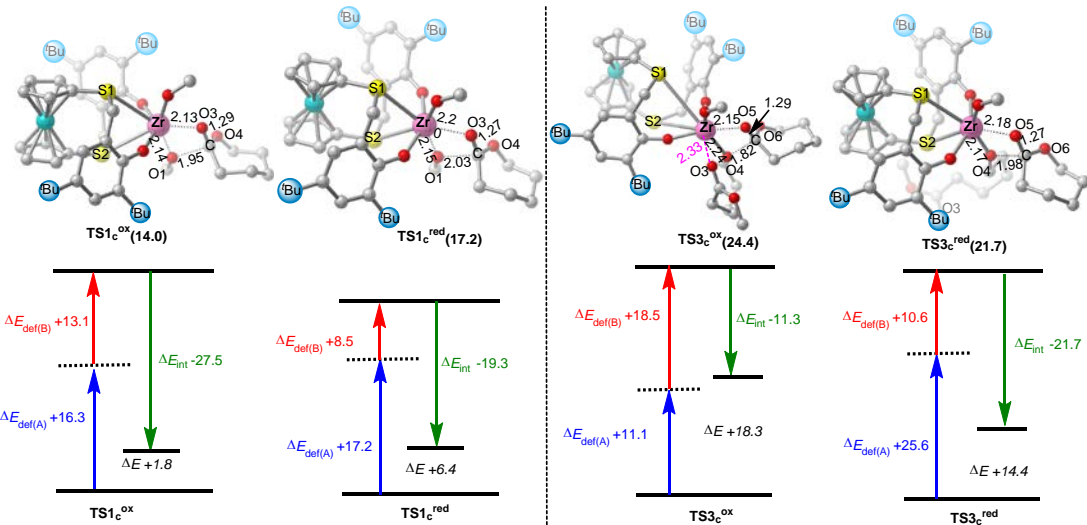


**Fig. S8** Optimized structures (distances in Å) and distortion/interaction analysis (kcal mol<sup>-1</sup>) of the four key transition states ( $\text{TS1}_c^{\text{ox}}$  vs  $\text{TS1}_c^{\text{red}}$ ,  $\text{TS3}_c^{\text{ox}}$  vs  $\text{TS3}_c^{\text{red}}$ ). Values in parentheses are the relative free energy barriers in solution (kcal mol<sup>-1</sup>).

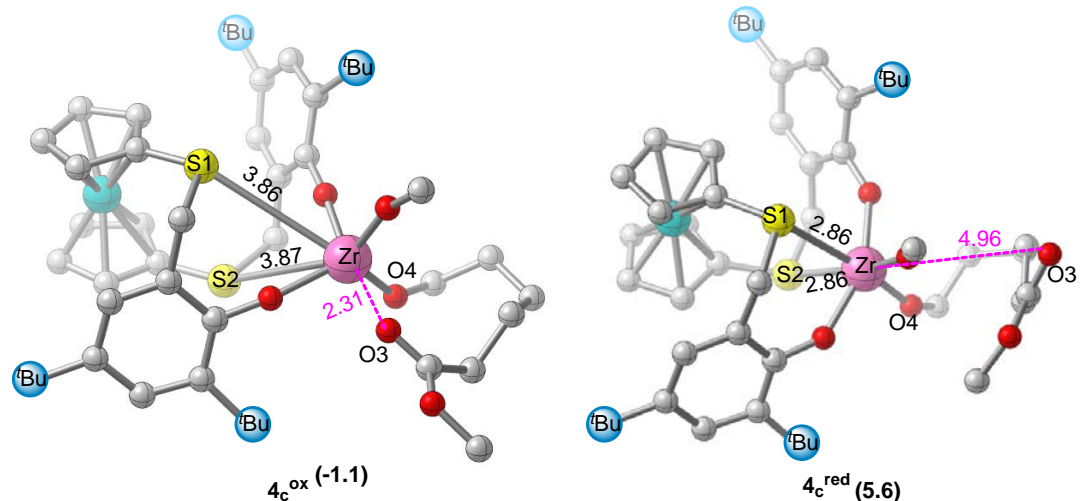


**Fig. S9** Optimized structure (distances in Å) and energy (kcal mol<sup>-1</sup>) of the insertion and ring-opening products  $4_c^{\text{ox}}$  and  $4_c^{\text{red}}$  of the first monomer. Values in parentheses are the relative Gibbs free energies (kcal mol<sup>-1</sup>) with respect to the sum of isolated reactants.

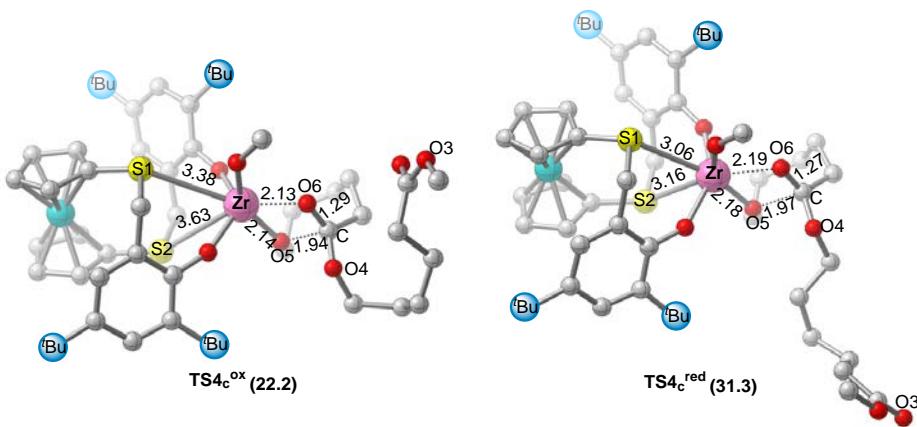


**Fig. S10** Optimized structures (distances in Å) of transition states  $\text{TS4}_\text{c}^\text{ox}$  and  $\text{TS4}_\text{c}^\text{red}$ . Values in parentheses are the relative Gibbs free energies (kcal mol<sup>-1</sup>) in solution with respect to isolated reactants.

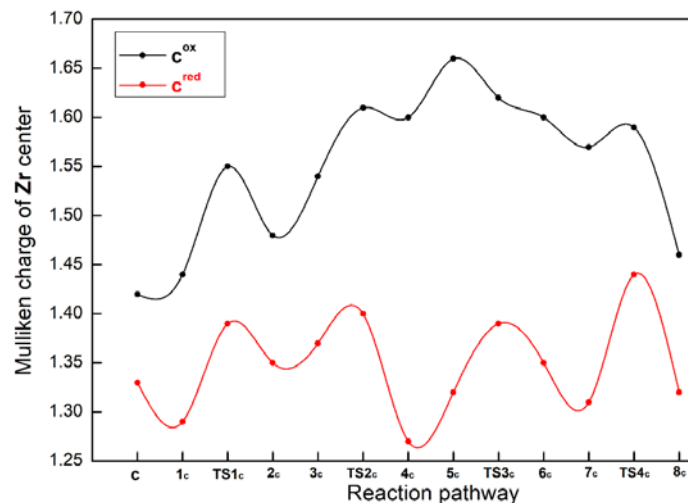


**Fig. S11** Mulliken charges on the catalytic metal center in the stationary points involved in the  $c^\text{ox}$  and  $c^\text{red}$  mediated reaction pathways.

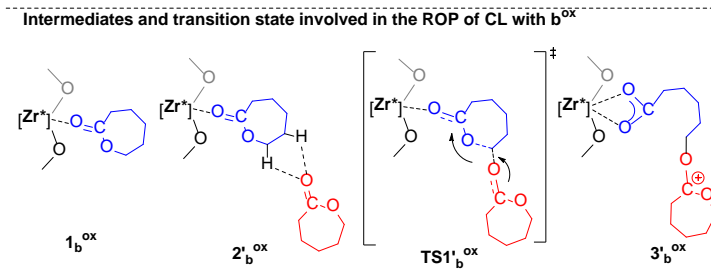
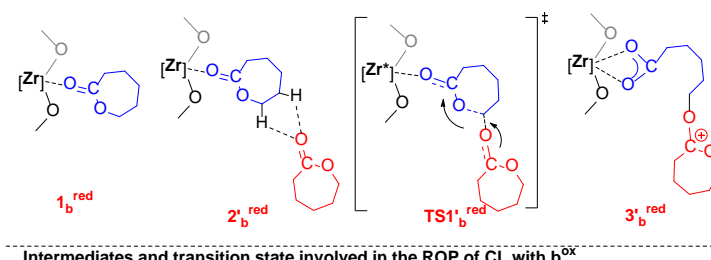
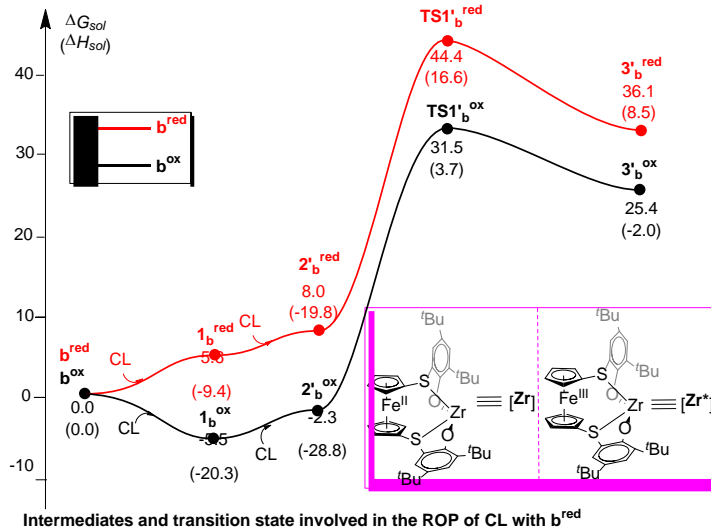
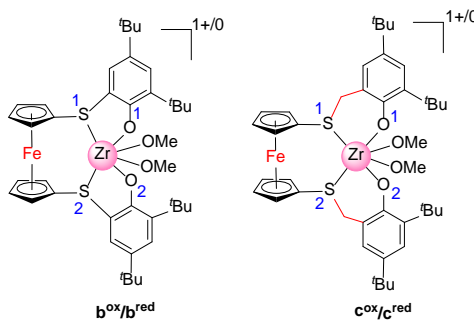


**Fig. S12** Free energy profiles for the possible pathway of ROP of CL with C=O bond cleavage mediated by **b<sup>ox</sup>** and **b<sup>red</sup>**.

**Table S1** Wiberg bond orders in **b<sup>red</sup>**, **c<sup>red</sup>**, **b<sup>ox</sup>**, and **c<sup>ox</sup>**.



	Zr-S1	Zr-S2	Zr-O1	Zr-O2	total
<b>b<sup>red</sup></b>	0.41	0.41	0.81	0.81	2.44
<b>c<sup>red</sup></b>	0.45	0.45	0.61	0.61	2.12
<b>b<sup>ox</sup></b>	0.08	0.08	0.22	0.22	0.60
<b>c<sup>ox</sup></b>	0.09	0.09	0.15	0.15	0.48

**Table S2** Relative electronic energies ( $\Delta E$ , kcal/mol) of various spin states of active species.

catalyst	spin states	$\Delta E$	catalyst	spin states	$\Delta E$
<b>a<sup>red</sup></b>	singlet (closed-shell)	0.0	<b>a<sup>ox</sup></b>	doublet	0.0
	singlet (open-shell)	0.0		quartet	16.3
	triplet	20.4		sextet	26.4
	quintet	19.4			
	septet	76.2			
<b>b<sup>red</sup></b>	singlet (closed-shell)	0.0	<b>b<sup>ox</sup></b>	doublet	0.0
	singlet (open-shell)	0.0		quartet	8.9
	triplet	34.6		sextet	17.8
	quintet	12.7			
	septet	91.8			
<b>c<sup>red</sup></b>	singlet (closed-shell)	0.0	<b>c<sup>ox</sup></b>	doublet	0.0
	singlet (open-shell)	0.0		quartet	15.5
	triplet	19.0		sextet	29.6
	quintet	18.2			
	septet	85.9			

### Examples of the input files

```
%chk=a_red.chk
%mem=8GB
%nproc=32
#p opt=(cartesian) freq=noraman ub3pw91/genecp EmpiricalDispersion=GD3
```

int

1 2			
Ti	-0.56714100	1.85893700	0.53939700
Fe	0.88255000	-2.65768700	-1.68406800
S	-0.12170500	-1.34893200	1.38945800
S	1.58201600	0.76481300	-2.04896500
...			
O	-0.57552200	3.00756000	-0.97854700
O	-0.78631300	3.76848200	1.32457800

C H O S 0

6-31G(d)

\*\*\*\*

Fe Ti 0

lanl2dz

\*\*\*\*

Fe Ti 0

lanl2dz

-----

```
%chk=TS1_red.chk
%mem=8GB
%nproc=24
#p opt=(calcfc,ts,cartesian,noeigentest) ub3pw91/genecp EmpiricalDispersion=GD3
freq=noraman
```

ts

1 2			
Ti	-0.56824600	1.83473500	0.58460500
Fe	0.87774000	-2.64571500	-1.70823800
S	-0.15523400	-1.38551900	1.38228500
S	1.61760500	0.77306000	-2.03839500
...			
O	-0.52383400	3.09241600	-0.92429500
O	-0.76116700	3.70175900	1.30211000

C H O S 0

6-31G(d)

\*\*\*\*

Fe Ti 0

lanl2dz

\*\*\*\*

Fe Ti 0

lanl2dz

---

```
%chk= TS1_red_s.chk
%mem=8GB
%nproc=24
#p um06/genecp scrf=(cpcm, solvent=benzene)
```

sp

1 2

Ti	-0.92878300	1.59215800	0.43882800
Fe	1.87471800	-2.46476300	-1.19753900
S	0.28651500	-1.09873600	1.60853200
S	1.36659000	0.85776200	-2.17937100
...			
O	-3.45683900	2.97849900	-0.42004300
O	-1.47870800	3.37635400	0.54665500

C H O S 0

6-311G(d,p)

\*\*\*\*

Ti Fe 0

MDF10

\*\*\*\*

Ti Fe 0

MDF10